

Electrically controlled strong coupling and polariton bistability in double quantum wellsChristopher Coulson,^{*} Gabriel Christmann, Peter Cristofolini, Cornelius Grossmann, and Jeremy J. Baumberg[†]
*Department of Physics, Cavendish Laboratory, University of Cambridge, Cambridge, CB3 0HE, United Kingdom*Simeon I. Tsintzos and George Konstantinidis
*Microelectronics Research Group, IESL-FORTH, P.O. Box 1527, 71110 Heraklion, Crete, Greece*Zacharias Hatzopoulos
*Microelectronics Research Group, IESL-FORTH, P.O. Box 1527, 71110 Heraklion, Crete, Greece
and Department of Physics, University of Crete, 71003 Heraklion, Crete, Greece*Pavlos G. Savvidis
*Microelectronics Research Group, IESL-FORTH, P.O. Box 1527, 71110 Heraklion, Crete, Greece
and Department of Materials Science and Technology, University of Crete, P.O. Box 2208, 71003 Heraklion, Greece*
(Received 16 March 2012; published 23 January 2013)

Direct electrical detection of the dispersion of electrically tuned light-matter strong coupling and consequent mapping of the polariton dispersion is achieved by tunneling photocurrent out of reverse-biased p - i - n microcavity structures. The coherent photon-assisted tunneling is based on mixing cavity photons into the electronic states. Associated with this double-quantum-well tunneling we demonstrate the optical bistability of polaritons maintained within the strong-coupling regime. An intrinsic hole population gates bistability through the local modulation of the potential profile produced by an optically controlled buildup of free carriers within the quantum wells.

DOI: [10.1103/PhysRevB.87.045311](https://doi.org/10.1103/PhysRevB.87.045311)

PACS number(s): 71.36.+c, 42.65.Pc, 73.63.-b, 78.67.-n

Using the coherent coupling of light and matter to alter the tunneling properties of electrons was first discussed during the 1960s when it was established that photons can optically excite an electron across an insulating gap between two superconductors.¹ As growth methods for nano- and mesoscale solid-state structures improved, schemes for photon-assisted tunneling (PAT) quickly developed. The oscillating electric field of a resonant photon modulates the local potential of an electronic state to modify its tunneling properties. Radiation applied to quantum wells or quantum dots dresses the electron energy levels, resulting in the emergence of Floquet states.² The resulting ladder of dressed states above and below the original energy provides new paths through which the electrons can tunnel.³⁻⁶

While these previous studies looked at the effect in tunneling of coupling light to a single electron or hole state, recently there has been interest in coupling to an excitonic state.⁷⁻⁹ The coherent mixing of light and matter modes in a semiconductor microcavity can result in the emergence of new eigenmodes called exciton polaritons. These are an admixture of light confined between two distributed Bragg reflectors (DBRs) and excitons confined within a quantum well.¹⁰ Their Bose statistics allows them to enhance a wide variety of nonlinear interactions, exhibiting enormous ultrafast amplification of light, nonlinear parametric amplification, and polariton condensation.¹¹⁻¹⁶

In this paper we demonstrate the direct measurement of the dispersion of electrically tuned light-matter strong coupling using the photocurrent (PC) of novel microcavity devices. The electronic states are dressed with cavity photons to form polaritons thus yielding a coherently assisted PAT. This allows the electrical mapping of polariton dispersions through the PC. Furthermore, while recent studies have observed

bistability of polaritons as they switch from the strong to weak coupling,¹⁷ we demonstrate a new version of polariton bistability maintained entirely within the strong-coupling regime. This bistability is caused by the modulation of the local potential around an asymmetric double-quantum well (ASDQW) due to the localization of excess internal charge. Similar to the bistability observed previously in ASDQWs,¹⁸ we extend our analysis to include charge buildup controlled by the electron and hole tunneling from the excitonic portion of the polariton states within an applied field. We find our model replicates the results and explains the unusual line shapes observed.

The excitonic modes of an ASDQW are coupled to the cavity mode of a microcavity [Fig. 1(a)]. The neighboring quantum wells separated by a tunneling barrier ($L = 4, 7, 20$ nm) support two excitons: the direct exciton (DX) has an electron and hole within the left quantum well (LQW), while the indirect exciton (IX) has a spatially separated electron localized in the right quantum well (RQW) and a hole in the LQW. These two excitons are coupled together with a tunnel splitting, J . The small overlap of the electron and hole wave functions in the IX produce a negligible oscillator strength. However, the DX is strongly coupled to the cavity photon mode with a Rabi splitting, Ω . Here we concentrate on a $L = 4$ nm sample in which $J \simeq \Omega \simeq 6$ meV. The Hamiltonian of the system is simply

$$H = \begin{pmatrix} \omega_{IX} & J/2 & 0 \\ J/2 & \omega_{DX} & \Omega/2 \\ 0 & \Omega/2 & \omega_C \end{pmatrix}. \quad (1)$$

Diagonalization of this gives three new eigenmodes: the upper, middle, and lower polaritons (UP, MP, and LP). When a

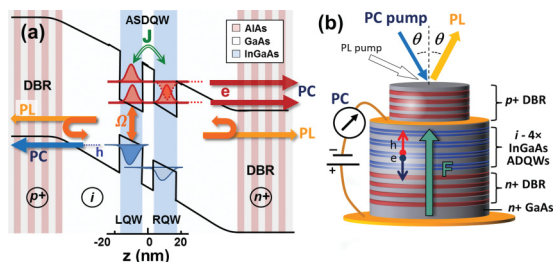


FIG. 1. (Color online) (a) Schematic band structure of microcavity p - i - n device, with eigenstates of ASDQW on resonance and relaxation routes for polaritons. J is the coupling between IX and DX; Ω is the coupling between DX and cavity modes. (b) Fabricated sample, showing angles of photocurrent excitation and photoluminescence collection.

bias is applied to the ASDQW the IX redshifts into resonance with the DX due to its dipole moment which is perpendicular to the QW plane. While the IX redshifts linearly with field, the DX weakly redshifts quadratically due to the quantum-confined Stark effect (QCSE) [Fig. 2(a)].¹⁹ Each polariton is composed of fractions of the uncoupled IX, DX, and C modes which change with applied field [Fig. 2(b)].

Photoexcited polaritons can relax through two channels. Either a fraction of the cavity photon tunnels through the DBR and is detected as photoluminescence or, under an applied bias, the excitonic component of the polariton can ionize when either an electron or hole tunnels out of the ASDQW generating a PC. Both the IX and DX contribute to the PC. While the wave function of the IX is localized in the RQW (so it has a shorter tunnel barrier), as soon as the DX is tuned

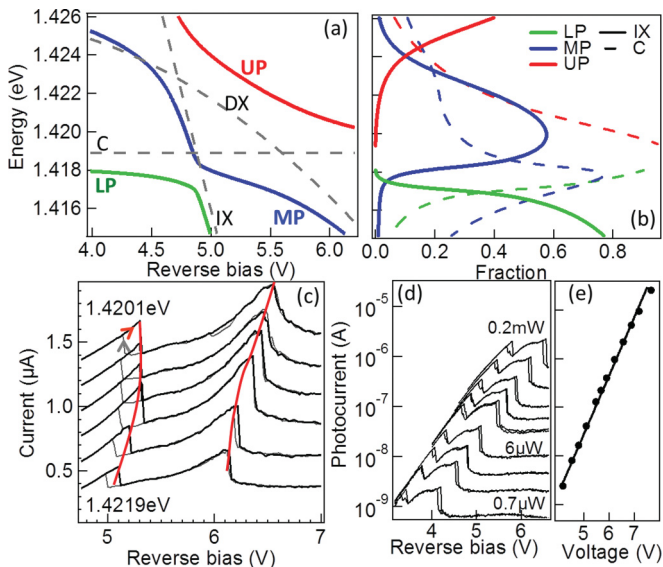


FIG. 2. (Color online) (a) Dispersion of polariton and uncoupled modes under applied reverse bias. (b) Decomposition of polariton into exciton ($X = IX + DX$) and cavity (C) components. (c) Photocurrents at increasing laser energies (as marked) sweeping in both negative and positive directions. Peaks correspond to strongly coupled modes redshifting into resonance. Excitation is $200 \mu\text{W}$. (d) Photocurrent at increasing laser powers with (e) extracted voltage and photocurrent at resonance for the different laser powers.

above the IX energy its smaller confinement energy results in a tunneling rate similar to the IX.

The strongly coupled $5\lambda/2$ -long undoped microcavity contains four sets of $\text{In}_{0.1}\text{Ga}_{0.9}\text{As}/\text{GaAs}/\text{In}_{0.08}\text{Ga}_{0.92}\text{As}$ ASDQWs placed at the antinodes of the electric field. The cavity is formed between a top (17-pair, p -doped) and bottom (21-pair, n -doped) GaAs/AlAs DBR thus forming a p - i - n junction [Fig. 1(b)]. The sample is processed into $400\text{-}\mu\text{m}$ diameter mesas with a ring-shaped Ti/Pt electrode deposited after a second etching step to the lower p -doped layers thus reducing series resistance.

Experiments are performed at 80 K in reverse bias with the PC excited by a tunable sub-GHz linewidth continuous wave (CW) Ti:sapphire laser at a variable angle θ . For the data here this angle is chosen as 35° to give a small negative detuning in combination with the appropriate temperature tuning, allowing the exciton modes to be bias tuned through the cavity mode. Photoluminescence (PL) is pumped at 50° by a CW Ti:sapphire laser tuned to 1.522 eV (above the cavity mirror stop band) and collected at 35° . Exciting the PC and collecting the PL at the same angle ensures they have the same detuning.

When pumping at a fixed laser energy the increasing bias redshifts the polariton modes into resonance. As each mode tunes toward resonance with the laser the absorption increases, causing a corresponding increase in the PC [Fig. 2(c)]. Changing the energy of the laser alters the voltage at which resonance is reached. Clear anticrossings in the modes observed in PC show the direct electrical control of the polariton modes [Fig. 2(c)].

The deviation of the IV curve from the expected Lorentzian line shape for polariton absorption [Fig. 2(c)] can be understood by considering the tunneling properties of the carriers, with rates given by $\tau_{e,h}^{-1} \propto \exp\{\sqrt{32}m_{e,h}^*U_{e,h}^3/3\hbar F\}$, where m^* is the effective mass, F is the applied field, and U is the confinement potential.²⁰ Within the GaAs barrier layer, the effective masses of the electron ($0.063m_e$) and hole ($0.51m_e$) set the base tunneling rate of the electrons to be orders of magnitude larger than that of the holes. This imbalance results in a large excess hole population within the LQW. The tunneling rates equilibrate as this excess positive charge modifies the potential profile around the ASDQW. This electrostatic interaction lowers the hole confinement energy, reducing tunneling time, and increases the electron confinement and tunneling time.

The polariton modes of the ASDQW thus experience an *effective field* across the wells, corresponding to the applied bias minus the opposing field of the holes. Increasing the bias shifts modes further into resonance, increasing both the electron tunneling rate and absorption. This further increases the imbalance between the electron and hole populations, maintaining an effective field which is lower than that of the applied field, and stretching the absorption spectrum. Once the mode has redshifted past resonance the absorption falls, reducing the hole population. This initiates positive feedback where the reduction in charging increases the effective field, further redshifting the mode away from resonance and further reducing the absorption. This causes the sharp drop in the PC beyond resonance.

In the reverse direction of voltage sweep, as the bias is lowered and the modes blueshift toward resonance, the inverse

process occurs. A small increase in the absorption leads to an increased hole population, decreasing the effective voltage causing a rapid blueshift toward resonance, and causing a step in the PC. The difference in position of the current step in the forward and reverse directions is a direct consequence of the hole buildup. In the forward direction the skewing of the absorption due to the excess hole population causes the peak absorption to occur at a higher applied bias than in the reverse direction, where the small absorption and high field lead to only a small hole excess. By comparing the voltage positions between the current step in forward and reverse directions it is possible to estimate the field due to the excess holes, giving typical hole densities of $3 \times 10^9 \text{ cm}^{-2}$, thus responsible for only a small reduction in DX oscillator strength.

An electric field, which opposes the applied field, exists between the separated charges contributing to the PC.²¹ This photovoltaic effect causes the electric field within the cavity to depend on the magnitude of the PC. It is useful, therefore, to correct the applied reverse bias V to eliminate these variable effects by converting to a scaled bias V' . The form of this scaling is confirmed through power-dependent experiments [Fig. 2(e)], and is given by

$$V' = V - V_0 \ln(I/I_0), \quad (2)$$

where (V_0, I_0) is a reference point on the PC.

Sweeping the voltage for a range of fixed laser energies produces a map of the polariton dispersion (Fig. 3). All three of the polariton modes from Fig. 2(a) are clearly visible, with a splitting of 3.5 meV between the UP and MP and 1.5 meV between the MP and LP. There is good agreement between the modes seen in the PL and in PC at low field. The white gaps in the PC represent the regions in which the rise in the hole population opposes the applied bias before the bistable transition. Also visible at high fields and high photon energies is the QCSE-shifted absorption associated with the DX of the RQW (not considered further). The dispersion calculated from

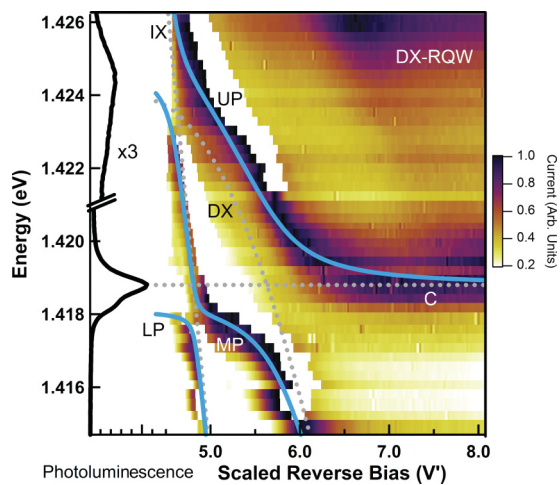


FIG. 3. (Color online) Map of photocurrent (with linear color scale, and normalized for each bias) on varying the laser tuning (eV) and effective reverse bias (V'). Lines show theory solution of polaritons (LP, MP, and UP) and uncoupled C, DX, and IX modes. White regions show jumps in hole charging. Left-hand graph shows photoluminescence at zero bias.

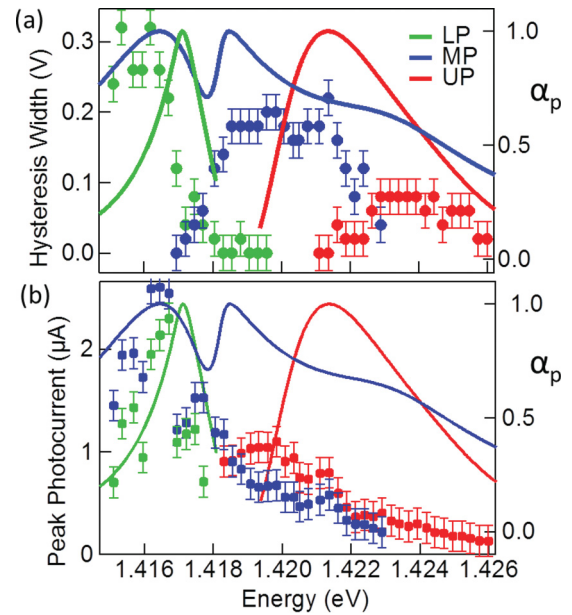


FIG. 4. (Color online) (a) Width of the hysteresis in bias for each polariton mode, and (b) the peak current at resonance. Lines show prediction from model of α_p (see text).

Eq. (1) tracks the experiment very well. Furthermore it is clear that the system remains in the strong-coupling regime despite the bistable effects.

The hysteresis is characterized by two quantities, the peak PC at resonance and the hysteresis width, defined as the difference in voltage of the forward and reverse current steps for each mode (Fig. 4). These two properties are linked since the width of hysteresis depends upon the magnitude of the excess

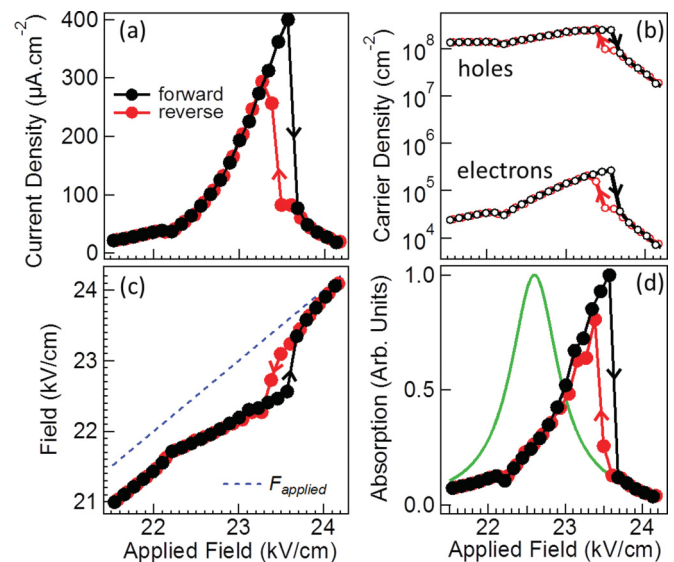


FIG. 5. (Color online) (a) Simulated IV characteristics of the ASDQW device under CW pumping in forward and reverse bias sweeps together with (b) the equilibrium density of electrons and holes in the ASDQW, (c) the effective field compared to the field applied across the ASDQW, and (d) the optical absorption of the mode corresponding to the photocurrent (green line shows the absorption with no charge buildup).

hole population. A larger hole population requires a higher bias to overcome the opposing field of the holes in order to reach resonance. Likewise the peak current flow is proportional to the electron and hole populations. The excess hole population of each polariton mode can be inferred from the predicted absorption based on multiplying the excitonic fraction by the cavity fraction $\alpha_P \propto (f_{IX} + f_{DX})f_C$ for each mode. This prediction successfully accounts for many aspects shown in the data (Fig. 4, lines) but fails most obviously for the MP when it is composed of all three light and matter components. Our explanation suggests that while strong coupling enhances the efficient injection of charge into the system, it is not a prerequisite for the observation of hysteresis in the ASDQW system. However, this estimate does not take into account many important features including the Coulomb binding of the excitons and the shake up in the energies after tunneling.

Full understanding of the bistable polaritons is produced through simulation of the carrier densities and tunneling rates. These two variables are linked: charge buildup changes the potential profile across the ASDQW, thus altering the tunneling times. These tunneling times in turn affect the population densities. Both Schrödinger and Poisson equations are thus solved iteratively using a finite difference method to provide the potential profile and eigenstates of the system.²² Combined with numerical solutions to the rate equations this produces equilibrium densities and tunneling times of the carriers. The absorption of the polariton mode is then calculated by solving Eq. (1). Simulations of the IV characteristics for a single polariton mode at a fixed laser energy [Fig. 5(a)] show clear hysteresis and mimic the experimental data well.

As the field increases the electron and hole populations increase [Fig. 5(b)]. Charge buildup near resonance then causes the effective voltage to diverge further from the applied voltage [Fig. 5(c)]. This dramatically alters the shape of the absorption curve [Fig. 5(d)]. In the forward direction the collapse in the hole population occurs at an effective field of 22.5 kV cm^{-1} , which agrees with the field for the peak absorption of the polariton without charge buildup [Fig. 5(d), green curve]. On the reverse sweep the collapse occurs at a lower field, resulting in switching at a smaller effective voltage below resonance, thus causing the hysteresis in the current.

In conclusion we have demonstrated the mapping of the dispersion of electrically tuned light-matter strong coupling through measurement of the PC of a microcavity. Bias-controlled polariton bistability is observed, due to intrinsic charge trapping in the ASDQW structure used to interface the mixed light-matter states with current transport. This, however, ensures the strong-coupling regime is not lost at any bias. Such schemes are suited to electrical control and measurement of coherent light-matter systems and open new opportunities in photon-assisted tunneling.

The authors acknowledge assistance from N. T. Pelekanos and support from Grants UKEPSRC (No. EP/G060649/ER) project, EU CLERMONT4 (No. PITNGA-2009235114), EU INDEX (No. FP7-2011-289968), EU FP7 IRSES “POLATER” project and Greek GSRT ARISTEIA “APOLLO” and “THALES NANOPHOS” programs.

*cc531@cam.ac.uk

†j.j.baumberg@phy.cam.ac.uk

¹A. Dayem and R. Martin, *Phys. Rev. Lett.* **8**, 246 (1962).

²F. Grossmann, T. Dittrich, P. Jung, and P. Hänggi, *Phys. Rev. Lett.* **67**, 516 (1991).

³M. Wagner, *Phys. Rev. A* **51**, 798 (1995).

⁴L. P. Kouwenhoven, S. Jauhar, J. Orenstein, P. L. McEuen, Y. Nagamune, J. Motohisa, and H. Sakaki, *Phys. Rev. Lett.* **73**, 3443 (1994).

⁵P. S. S. Guimaraes, B. J. Keay, J. P. Kaminski, S. J. Allen, P. F. Hopkins, A. C. Gossard, L. T. Florez, and J. P. Harbison, *Phys. Rev. Lett.* **70**, 3792 (1993).

⁶T. C. L. G. Sollner, W. D. Goodhue, P. E. Tannenwald, C. D. Parker, and D. D. Peck, *Appl. Phys. Lett.* **43**, 588 (1983).

⁷D. Bajoni, E. Semenova, A. Lemaître, S. Bouchoule, E. Wertz, P. Senellart, and J. Bloch, *Phys. Rev. B* **77**, 113303 (2008).

⁸T. A. Fisher, A. M. Afshar, D. M. Whittaker, M. S. Skolnick, J. S. Roberts, G. Hill, and M. A. Pate, *Phys. Rev. B* **51**, 2600 (1995).

⁹L. Sapienza, A. Vasanelli, C. Ciuti, C. Manquest, C. Sirtori, R. Colombelli, and U. Gennser, *Appl. Phys. Lett.* **90**, 201101 (2007).

¹⁰C. Weisbuch, M. Nishioka, A. Ishikawa, and Y. Arakawa, *Phys. Rev. Lett.* **69**, 3314 (1992).

¹¹P. G. Savvidis, J. J. Baumberg, R. M. Stevenson, M. S. Skolnick, D. M. Whittaker, and J. S. Roberts, *Phys. Rev. Lett.* **84**, 1547 (2000).

¹²R. M. Stevenson, V. N. Astratov, M. S. Skolnick, D. M. Whittaker, M. Emam-Ismael, A. I. Tartakovskii, P. G. Savvidis, J. J. Baumberg, and J. S. Roberts, *Phys. Rev. Lett.* **85**, 3680 (2000).

¹³C. Diederichs, J. Tignon, G. Dasbach, C. Ciuti, A. Lemaître, J. Bloch, Ph. Roussignol, and C. Delalande, *Nature (London)* **440**, 904 (2006).

¹⁴M. Saba, C. Ciuti, J. Bloch, V. Thierry-Mieg, R. André, L. S. Dang, S. Kundermann, A. Mura, G. Bongiovanni, J. L. Staehli, and B. Deveaud, *Nature (London)* **414**, 731 (2001).

¹⁵J. Kasprzak, M. Richard, S. Kundermann, A. Baas, P. Jeambrun, J. M. J. Keeling, F. M. Marchetti, M. H. Szymanska, R. André, J. L. Staehli, V. Savona, P. B. Littlewood, B. Deveaud, and Le Si Dang, *Nature (London)* **443**, 409 (2006).

¹⁶R. Balili, V. Hartwell, D. Snoke, L. Pfeiffer, and K. West, *Science* **316**, 1007 (2007).

¹⁷D. Bajoni, E. Semenova, A. Lemaître, S. Bouchoule, E. Wertz, P. Senellart, S. Barbay, R. Kuszelewicz, and J. Bloch, *Phys. Rev. Lett.* **101**, 266402 (2008).

¹⁸R. Ferreira, P. Rolland, Ph. Roussignol, C. Delalande, A. Vinatteria, L. Carraresi, M. Colocci, N. Roy, B. Sermage, J. F. Palmier, and B. Etienne, *Phys. Rev.* **45**, 11782 (1992).

¹⁹D. A. B. Miller, D. S. Chemla, T. C. Damen, A. C. Gossard, W. Wiegmann, T. H. Wood, and C. A. Burrus, *Phys. Rev. Lett.* **53**, 2173 (1984).

²⁰G. Bastard, J. A. Brum, and R. Ferreira, *Semiconductor Heterostructures and Nanostructures* (Elsevier, New York, 1991).

²¹R. L. Cumberow, *Phys. Rev.* **95**, 16 (1954).

²²I. H. Tan, G. L. Snider, L. D. Chang, and E. L. Hu, *J. App. Phys.* **68**, 4071 (1990).